Simulation study on the influence of longitudinal dynamic force on extreme-long heavy-haul trains

Chongyi Chang, Gang Guo and Wen He

Railway Science and Technology Research and Development Center,
China Academy of Railway Sciences Corporation Limited, Beijing, China, and

Zhendong Liu

Department of Engineering Mechanics, KTH Royal Institute of Technology,
Stockholm, Sweden

Abstract

Purpose – The objective of this study is to investigate the impact of longitudinal forces on extreme-long heavy-haul trains, providing new insights and methods for their design and operation, thereby enhancing safety, operational efficiency and track system design.

Design/methodology/approach – A longitudinal dynamics simulation model of the super long heavy haul train was established and verified by the braking test data of 30,000 t heavy-haul combination train on the long and steep down grade of Daqing Line. The simulation model was used to analyze the influence of factors on the longitudinal force of super long heavy haul train.

Findings – Under normal conditions, the formation length of extreme-long heavy-haul combined train has a small effect on the maximum longitudinal coupler force under full service braking and emergency braking on the straight line. The slope difference of the long and steep down grade has a great impact on the maximum longitudinal coupler force of the extreme-long heavy-haul trains. Under the condition that the longitudinal force does not exceed the safety limit of 2,250 kN under full service braking at the speed of 60 km/h the maximum allowable slope difference of long and steep down grade for 40,000 t super long heavy-haul combined trains is 13‰, and that of 100,000 t is only 5‰.

Originality/value – The results will provide important theoretical basis and practical guidance for further improving the transportation efficiency and safety of extreme-long heavy-haul trains.

Keywords Heavy-haul combined train, Longitudinal dynamics, Train length,
Locomotive synchronization control, Slope difference

Paper type Research paper

1. Introduction

As the development of world railway freight continues, improving transportation efficiency, reducing energy consumption and optimizing transportation costs have become increasingly important goals. In the process of achieving these goals, the operation of extreme-long heavy-haul trains is considered an effective approach. The operation of extreme-long trains is an effective way to increase heavy-haul transportation capacity. By increasing axle load and expanding train length, extreme-long heavy-haul trains can transport more goods in a single

trip, thus improving transportation efficiency. However, the force situation of extreme-long heavy-haul trains is more complex than that of general trains, and the impact law of longitudinal forces needs to be studied in depth.

For coal transport in China, the trains with a traction mass over 40,000 t are called extreme-long trains, which can effectively increase the transport capacity. Datong–Qinhuangdao heavy-haul railway in China has 20,000 t heavy-haul combined trains in operation and has conducted operational test of 30,000 t heavy-haul trains (Yao, 2014). Extreme-long trains over 40,000 t heavy are in operation in South Africa and Australia. For example, Australia completed the operational test of 99,700 t heavy-haul trains in 2001 (Cole, 2006). However, as the application of extreme-long heavy-haul trains is being promoted, the force situation becomes more complex, especially for 40,000 t or even 100,000 t extreme-long trains and the impact law of longitudinal forces is not yet clear. Therefore, studying the impact law of longitudinal forces in extreme-long heavy-haul trains is of great significance and can further promote the development of heavy-haul transportation.

In the research of the impact law of longitudinal forces in extreme-long heavy-haul trains, simulation studies of longitudinal dynamics have become an important means. Through simulation calculations, the magnitude and distribution of longitudinal forces under different operating conditions can be analyzed, providing scientific basis for the safety design and operation of trains. In addition, simulation studies can optimize the design and operation strategies of trains; improve energy efficiency and operational efficiency. Therefore, the necessity of simulation research on the impact law of longitudinal forces in extreme-long heavy-haul trains is self-evident. The key technologies and methods of the longitudinal dynamics simulation are discussed in references Chang *et al.* (2016, 2017), Wu *et al.* (2014, 2016), Wu *et al.* (2018) and Yang *et al.* (2010).

However, simulation research on the impact law of longitudinal forces in extreme-long heavy-haul trains faces some challenges. Firstly, the force situation of extreme-long heavy-haul trains is more complex, requiring the establishment of accurate simulation models. Secondly, the impact law of longitudinal forces involves in-depth exploration of train dynamics and mechanics, requiring innovation and development of relevant technologies. In addition, simulation research needs to consider the variation law of longitudinal forces under different operating conditions, further improving the safety of trains, operational efficiency and track system design.

The goal of this research is to study the impact law of longitudinal forces in extreme-long heavy-haul trains in depth. Through simulation and modeling, we can reveal the longitudinal dynamic characteristics and mechanical behavior of extreme-long heavy-haul trains and solve key technical problems that may be encountered in actual operations. This will provide new ideas and methods for the design and operation of extreme-long heavy-haul trains, thereby improving the safety, operational efficiency and track system design. To achieve this goal, this research will use the simulation methods, combined with actual operational data and field test verification, to systematically study the longitudinal dynamic characteristics and mechanical behavior of extreme-long heavy-haul trains. This research will provide important theoretical basis and practical guidance for further improving the transportation efficiency and safety of extreme-long heavy-haul trains.

2. Modelling
2.1 Multi-mass model on train longitudinal dynamics
The longitudinal dynamic model of extreme-long trains is mainly used to analyze the longitudinal dynamics action between locomotives and vehicles with respect to different train formations, wireless synchronous control of the distributed locomotives, operational strategies, running conditions and the line profile. The main characteristics of the longitudinal dynamic model of the extreme-long train are that the train length is long, the degree of freedom (DOF) is

large and the longitudinal force transmission is complex. In the present model, every single locomotive or vehicle is used as a rigid body and the DOF of the extreme-long train is equal to the total number of vehicles (i.e. locomotives and rolling stocks), as shown in Figure 1. In the figure: m_i is the mass of the ith vehicle; u_i is the displacement of the ith vehicle; the n in m_{hn} is the number of vehicles in each unit; the h in m_{hn} is the hth unit in train groups.

Equation of longitudinal dynamics for the extreme-long train (cf. Figure 1) can be expressed as

$$m_i\ddot{u}_i = F_{ci-1} - F_{ci} - F_{wi} - F_{TEi} - F_{DBi} - F_{Bi} \tag{1}$$

Where m_i is the mass of the i vehicle; u_i is the displacement of the i vehicle; $\ddot{u}_i$ is the acceleration of the ith vehicle; F_{ci-1} is the anterior coupler force of the i vehicle, $F_{c0-1} = 0$; F_{ci} is the posterior coupler force of the i vehicle, $F_{ckn} = 0$; F_{wi} is the total running resistance of the ith vehicle, including equivalent running resistance, ramp resistance, curve resistance, starting resistance and so on; F_{TEi} is the locomotive tractive force; F_{DBi} is the locomotive dynamics braking force; F_{Bi} is the air braking force of the ith vehicle. In Eq. (1), there are

$$F_{ci-1} = \widetilde{k}_{i-1}(u_i - u_{i-1}) \tag{2}$$

$$F_{ci} = \widetilde{k}_i(u_{i+1} - u_i) \tag{3}$$

Where $\widetilde{k}_{i-1}$ is the instantaneous stiffness of the anterior draft gear of the ith vehicle in series with the posterior draft gear of the adjacent vehicle and $\widetilde{k}_i$ is the instantaneous stiffness of the posterior draft gear of the ith vehicle in series with the anterior draft gear of the adjacent vehicle. Substituting Eq. (2) and Eq.(3) into Equation (1) results in to:

$$\begin{cases} \mathbf{M\ddot{u}} + \widetilde{\mathbf{K}}\mathbf{u} = \mathbf{F} \\ \dot{\mathbf{u}}|_{t=0} = \mathbf{v}_0 \\ \mathbf{u}|_{t=0} = \mathbf{u}_0 \end{cases} \tag{4}$$

Where M is the mass matrix of rolling stocks; $\widetilde{\mathbf{K}}$ is the instantaneous total nonlinear stiffness matrix of the system; F is the additional stimulation of the train system; $\ddot{\mathbf{u}}$, $\dot{\mathbf{u}}$ and $\mathbf{u}$ are the acceleration, velocity and longitudinal displacement generalized coordinate vector of the model.

2.2 Air brake model
Traditional brake shoe braking is widely used on the Chinese heavy-haul trains. The compressed air is motive power of brake; braking force is generated by the friction force between the brake shoe and the wheel caused by air brake controlling brake shoe pressing the wheel tread. The brake force can be expressed as

$$F_B = 1000 \sum K \cdot \phi_k \tag{5}$$

Where K is the brake shoe pressure, ϕ_k is the friction coefficient of brake shoe.
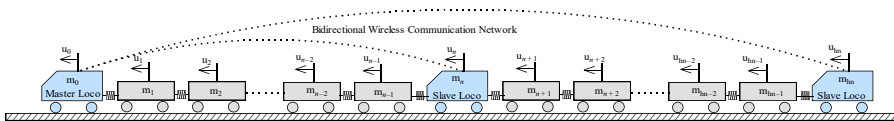
Source(s): Authors own work

Brake shoe pressure K is expressed as following equation (Kaiwen, 1990):

$$K = \frac{\pi}{4}d^2 \cdot p_{BC} \cdot \eta \cdot \gamma \cdot n_b \cdot 10^{-3} \qquad (6)$$

Where π is the circumference ratio, d is the diameter of brake cylinder (mm), p_{BC} is the pressure of brake cylinder (kPa), η is the transmission efficiency of foundation brake rigging, γ is the braking leverage, n_b is the number of brake cylinders.

After the diameter of brake cylinder and foundation brake rigging is determined, air brake force depends on friction coefficient of brake shoe ϕ_k and pressure of brake cylinder p_{BC}.

Friction coefficient of brake shoe ϕ_k is related to the material properties, pressure of brake shoe and running speed. Friction coefficient of high friction composite brake shoe ϕ_k is expressed as the following equation (Regulations on Railway Train Traction Calculation, 1998).

$$\phi_k = 0.41 \cdot \frac{K+200}{4K+200} \cdot \frac{v+150}{2v+150} \qquad (7)$$

Where v is the running speed (km/h).

Pressure of brake cylinder p_{BC} is related to the brake characteristic, the vehicle site in train, pressure decrement of train brake pipe, etc. Pressure of brake cylinder p_{BC} is expressed as

$$p_{BC}^i = f\left(t_b, p_0^i, \Delta p\right) \qquad (8)$$

Where i is the vehicle site in train, p_{BC}^i is the brake cylinder pressure of the i vehicle (kPa), t_b is the brake time of the i vehicle and star from the brake cylinder pressure of the vehicle beginning ascend (s), p_0^i is the pressure of train pipe of the i vehicle in release state (kPa), Δp is pressure decrement of train pipe (kPa).

The empirical formula of train pipe pressure distribution of the i vehicle is obtained by curving fitting for measured data of the change curve of train pipe pressure in brake test. The pressure of train pipe p_0^i is expressed as

$$p_0^i = f(p_0, N, i) \qquad (9)$$

Where p_0 is the fixed air pressure of train pipe (500kPa or 600kPa), N is the vehicle number of train.

First, two different brake wave propagation speeds of train pipe are assumed for service and emergency brakes, respectively. Based on 0 time when the brake command is sent from the locomotive, the starting ascend time of brake cylinder pressure of the i vehicle t_p^i, which is expressed as

$$t_p^i = a \cdot N_L - b \cdot c \cdot e \qquad (10)$$

Where N_L is the number of locomotives in train, $e = (i+1) - d$, a, b, c and d values are related to the braker type. For emergency brake case of 120 type brake used in China, $a = -0.45 - N_L \cdot 0.4$, $b = 0.07$, $c = 1.0$, $d = 1.0$.

2.3 Dynamics characteristics model of coupler and draft gears

One of the main characteristics of the train longitudinal dynamics simulation different from the simple traction calculation is that the former calculates all the coupler forces and accelerations of the rolling stocks. Therefore, the coupling slack changes and the series resistance characteristics of draft gear combination must be considered. According to the

equipment conditions of heavy-haul train, this model is mainly based on the simulation of the steel friction type draft gear (MT-2) in China. The following mathematical equation which was used to describe the suspension forces in the suspension system (Fancher *et al.*, 1980) is mainly used into draft gear model.

$$F_t = FENV_t + (F_{t-\Delta t} - FENV_t)exp\left(\frac{-|x_t - x_{t-\Delta t}|}{\beta}\right) \tag{11}$$

F_t is coupler force in current time step; $FENV_t$ is force of upper and lower sideline.

$$FENV_t = \begin{cases} f(x_t) + f_{adh}\left(x_t, \dot{x}_t\right) + cf(b - x_t)\dot{x}_t^{nf} \text{when } x_t > x_{t-\Delta t} \\ kx_t - F_b \text{when } x_t < x_{t-\Delta t} \end{cases} \tag{12}$$

$F_{t-\Delta t}$ is the coupler force in preceding time step; x_t is the deformation of coupler and draft gears in current time step; $x_{t-\Delta t}$ is the deformation of coupler and draft gears in preceding time step; β is the parameter to control the changing rate of the connecting line between loading and unloading force sideline, which has the same unit to x and whose value should be selected according to the test diagram of draft gears.

$f(x_t)$ is the fitting function of dynamic loading characteristic curve from resistance force and stroke which are obtained through a large graft gear impact test. F_b is the initial pressure of graft gear; k is the stiffness of the elastic element in graft gear. cf is the speed-dependent damping coefficient; nf is the speed factor; b is the compressive deflection from pre-pressure.

The HM-1 draft gear is an elasticity cement and steel-friction type composite draft gear and the damping effect of steel friction and elasticity cement is considered in this draft gear model. When the relative speed of steel friction mechanism is less than the viscous critical speed of steel friction in the process of draft gear loading, additional viscous friction (Sun *et al.*, 2015) can be expressed as

$$f_{adh}\left(x, \dot{x}\right) = f(x_t) \cdot \left(v_c - \left|\dot{x}\right|\right) \cdot \frac{(\mu_s - \mu_k)}{v_c} \tag{13}$$

Where μ_s and μ_k are the equivalent static and dynamic friction coefficient of steel friction mechanism in draft gear; v_c is the viscous critical speed of steel friction.

The fitting function $f(x_t, \dot{x}_t)$ of dynamic loading characteristics curve of numerical model for friction draft gear shall contain the steel frictional dynamic loading characteristics of the loading curve, additional viscous friction and speed damping force.

2.4 Numerical solution of longitudinal dynamics equations of heavy-haul train

Longitudinal dynamics equation of train is a very complicated nonlinear equation, which includes many nonlinear factors such as the nonlinear impedance characteristics; coupler clearance, nonlinear working characteristics of traction and braking. Direct numerical integration is mainly applied to solve it. Dynamical response of direct numerical integration method in engineering application can be divided into two categories: explicit form and implicit form. Mostly, implicit methods include Newmark-β method, Wilson-θ method and Houbolt method; and explicit methods widely used, beside central difference method and modified cyclic iteration method based trapezoidal rule, include Newmark fast-display integration method and a kind of prediction-correction integration method (Zhai, 1990, 1996).

Newmark-β method is one of the numerical integration methods which are widely used for its high precision. It suits for the solution of linear vibration system balance equation. The mathematical expression is,

$$M_{t+\Delta t}\ddot{u}_{t+\Delta t} + K_{t+\Delta t}u_{t+\Delta t} = F_{t+\Delta t} \tag{14}$$

This method introduces the relation between speed and displacement as follows (Newmark, 1959):

$$u_{t+\Delta t} = u_t + \Delta t\dot{u}_t + \left(\frac{1}{2} - \beta\right)\Delta t^2\ddot{u}_t + \beta\Delta t^2\ddot{u}_{t+\Delta t} \tag{15}$$

$$\dot{u}_{t+\Delta t} = \dot{u}_t + (1-\gamma)\Delta t\ddot{u}_t + \gamma\Delta t\ddot{u}_{t+\Delta t} \tag{16}$$

β and γ are variable parameters, which are used to adjust the calculation characteristics of the formula especially the adjustment of its stability and precision.

$$\left(M_{t+\Delta t} + K_{t+\Delta t}\beta\Delta t^2\right)\ddot{u}_{t+\Delta t} = F_{t+\Delta t} - K_{t+\Delta t}\left(u_t + \Delta t\dot{u}_t + \left(\frac{1}{2} - \beta\right)\Delta t^2\ddot{u}_t\right) \tag{17}$$

Assuming u_t, $\dot{u}_t$ and $\ddot{u}_t$ can be calculated on the preceding step, after the institution, $\ddot{u}_{t+\Delta t}$ is obtained. Then $\dot{u}_{t+\Delta t}$ and $u_{t+\Delta t}$ at can be obtained according to Formula (15) and (16). In order to imply step-by-step integration method into the response calculation of nonlinear equation, this equation solution is changed into the iterative solution within each time step Δt. Now the increment balance formula of differential equation can be written as:

$$M_t\Delta\ddot{u}_t + K_T(\Delta u_t) = \Delta F_t \tag{18}$$

Where K_T is the stiffness matrix, which is defined as

$$K_T = \left(\frac{\partial F_s}{\partial u}\right)_t \tag{19}$$

F_s is the force vector of vibration system to resist deformation.

Just at the time $t + \Delta t$, equation can be written as

$$M\ddot{u}_{t+\Delta t} + K_T(\Delta u_t) = F_{t+\Delta t} - F_t + M\ddot{u}_t \tag{20}$$

In terms of the strong nonlinear vibration, to reduce errors, equilibrium iteration is commonly used for solving discrete nonlinear equation in a small increase step. Since K_T is changing in the iteration process, approximate solution would not be obtained until it changes into the final balance condition. We use the linear result as the first approximate to calculate its following imbalance force, and then take this force into the vibration system to get a new linear result, which is used to the second approximate and calculate the following imbalance force, and then take the second imbalance force into the vibration system to get the linear result, which is used to the third approximate and calculate the following imbalance force. Repeat this iteration, till the imbalance force eliminated.

To achieve the iteration calculation mentioned above, the initial value of $u_{t+\Delta t}$ and $\dot{u}_{t+\Delta t}$ shall be provided. If the provision of the initial value is not proper, it is no doubt that the iteration times would be increased. So the initial value can be obtained by Newmark explicit integration form (Zhai, 1996).

$$u_{t+\Delta t}^{(0)} = u_t + \Delta t\dot{u}_t + \left(\frac{1}{2} + \psi\right)\Delta t^2\ddot{u}_t - \psi\Delta t^2\ddot{u}_{t-\Delta t} \tag{21}$$

$$\dot{\boldsymbol{u}}_{t+\Delta t}^{(0)} = \dot{\boldsymbol{u}}_t + (1+\phi)\Delta t \ddot{\boldsymbol{u}}_t - \phi \Delta t \ddot{\boldsymbol{u}}_{t-\Delta t} \tag{22}$$

$\boldsymbol{u}_{t+\Delta t}^{(0)}$ and $\dot{\boldsymbol{u}}_{t+\Delta t}^{(0)}$ can be predicted by Formula (19) and (14), and $\boldsymbol{K}_T^{(0)}$ can be obtained. According the balance equation in incremental form, the formula below can be obtained:

$$\boldsymbol{M} \ddot{\boldsymbol{u}}_{t+\Delta t}^{(1)} + \boldsymbol{K}_T^{(0)} \left(\Delta \boldsymbol{u}_t^{(0)} \right) = \boldsymbol{F}_{t+\Delta t} - \boldsymbol{F}_t + \boldsymbol{M} \ddot{\boldsymbol{u}}_t \tag{23}$$

With formula (21), $\ddot{\boldsymbol{u}}_{t+\Delta t}^{(1)}$ is calculated. With Formula (13) and (8), $\boldsymbol{u}_{t+\Delta t}^{(1)}$ and $\dot{\boldsymbol{u}}_{t+\Delta t}^{(1)}$ are calculated. Then recalculate $\boldsymbol{K}_T^{(1)}$ with Formula (17), thus imbalance force $\Delta \widetilde{\boldsymbol{F}}^{(1)}$ can be calculated with Formula (24) and (25).

$$\boldsymbol{M} \ddot{\boldsymbol{u}}_{t+\Delta t}^{(1)} + \boldsymbol{K}_T^{(1)} \left(\Delta \boldsymbol{u}_t^{(1)} \right) = \widetilde{\boldsymbol{F}}^{(1)} \tag{24}$$

$$\Delta \widetilde{\boldsymbol{F}}^{(1)} = \boldsymbol{F}_{t+\Delta t} - \boldsymbol{F}_t + \boldsymbol{M} \ddot{\boldsymbol{u}} - \widetilde{\boldsymbol{F}}^{(1)} \tag{25}$$

Let imbalance force $\Delta \widetilde{\boldsymbol{F}}^{(1)}$ act on the instantaneous vibration system and solve the balance equation:

$$\left(\boldsymbol{M} + \boldsymbol{K}_T^{(1)} \beta \Delta t^2 \right) \Delta \ddot{\boldsymbol{u}}_{t+\Delta t}^{(2)} = \Delta \widetilde{\boldsymbol{F}}^{(1)} \tag{26}$$

The second approximate value is obtained as:

$$\ddot{\boldsymbol{u}}_{t+\Delta t}^{(2)} = \ddot{\boldsymbol{u}}_{t+\Delta t}^{(1)} + \Delta \ddot{\boldsymbol{u}}_{t+\Delta t}^{(2)} \tag{27}$$

The iteration cannot be ended until it satisfies the balance rule $\left\| \Delta \overline{\boldsymbol{F}}^{(n)} \right\| < \varepsilon$ according to such repeated calculation. Therefore, one step of integral is finished and then continue to the next step with $\ddot{\boldsymbol{u}}_{t+\Delta t}^{(n)}$ as its initial value.

The calculation of unit basic running resistance, gradient resistance and curve resistance for the train are referred to the Chinese Regulations on Railway Train Traction Calculation (1998).

For extreme-long train, the locomotives are distributed at different positions along the train. The wireless synchronous control technology is used between the master and slave locomotives in the group. The operation control model is based on LOCOTROL synchronization proposed in the reference Chang *et al.* (2017).

3. Verification
The longitudinal dynamics equation of extreme-long trains is a nonlinear problem, which includes many nonlinear factors, such as the nonlinear resistance of the draft gear and the nonlinear traction and braking curve. The high precision equilibrium iterative method based on the Newmark-β (Chang *et al.*, 2017) is used to solve the longitudinal dynamics of the extreme-long train. The algorithm which has been verified by a line test has been applied to obtain the longitudinal force of a 20,000 t heavy-haul train during emergency braking in reference Chang *et al.* (2017).

In order to validate the present model under cycle braking condition on long and steep downhill track section, a simulation is carried out according to the test condition of a 30,000 t train on Datong–Qinhuangdao Line (up to now, the longest heavy-haul train of the line tests in China). The simulation is then compared against the measurement of the test for validation. The 30,000 t train is composed of three HX$_D$1-type locomotives, a SS4-type locomotive and

315 C_{80}-type wagons according to the distributed power mode. The test locomotives are equipped with LOCOTROL wireless synchronous control system, No.13 couplers and MT-3 type draft gears; every three wagons are assembled with traction rods and form a group. The wagon groups are connected with No.16 and No.17 couplers (with a coupler clearance of 24 mm) and equipped with 120-type brake and MT-2 type draft gear. Formation of the test train: HX_D1 (master locomotive) + 105 × C_{80} + HX_D1 (slave locomotive No.1) + 105 × C_{80} + HX_D1 (slave locomotive No.2) + 105 × C_{80} + SS4 (slave locomotive No.3). Operational parameters of the 30,000 t test train on the long and steep downhill section are shown in Figure 2.

The braking and longitudinal dynamic parameters of the vehicle by arranging 15 measuring sections in the 30,000 t test train are tested, each 105 wagons forms a unit train group a wagon unit. Measurement takes place at the 1st, 25th, 52nd, 79th and 103rd/105th wagon in each wagon unit. The measured information includes coupler forces, longitudinal acceleration of the vehicles, main braking pipe pressure, auxiliary reservoir pressure and braking cylinder pressure. The test of grade braking is carried out when the test train runs at 70 km/h at Point K288 + 320 (grade − 10‰) of the Line. In the test, the synchronous response time between the master locomotive at the head of the train and the three slave locomotives is monitored in real-time. The results show that the action time of the three slave locomotives is 2–3 s delay after the master locomotive.

The operation information of 30,000 t test train on the long and steep downhill line is shown in Figure 2.

A comparison of the measured longitudinal force at couplers and simulation results (the 53rd, 104th, 131st, 164th and 280th vehicle) are made in Figure 3. It can be seen that the simulation is close to the measurement, which proves that the numerical model and algorithm shown in Section 2 can be used to calculate the longitudinal force of 30,000 t trains.
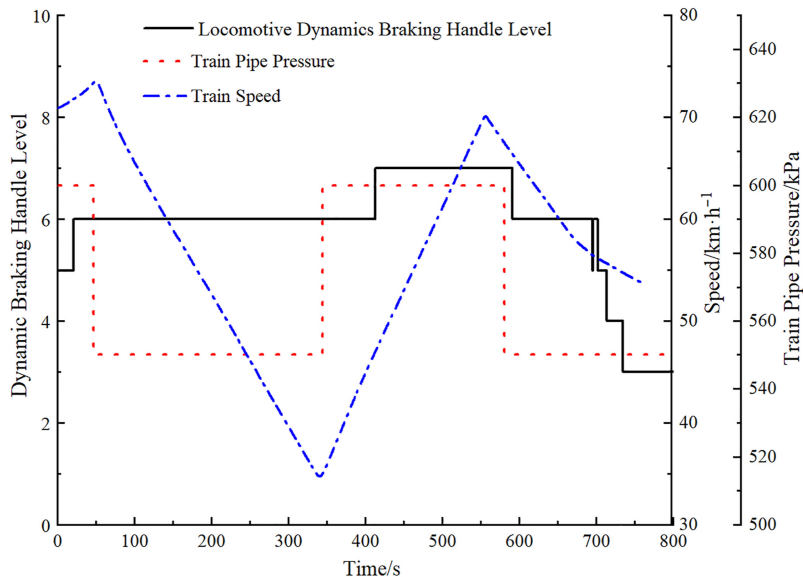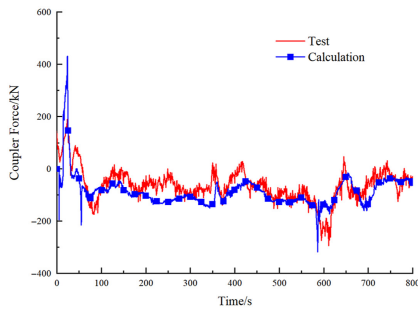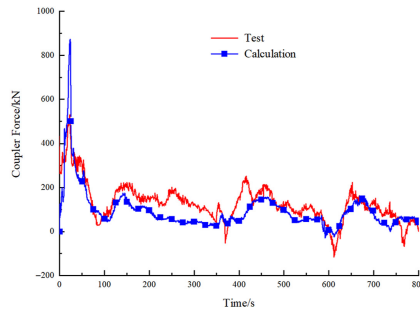

Figure 2.
The operation of 30,000 t test train on the long and steep downhill section
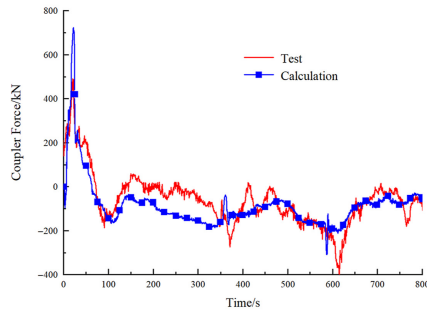
Source(s): Authors own work

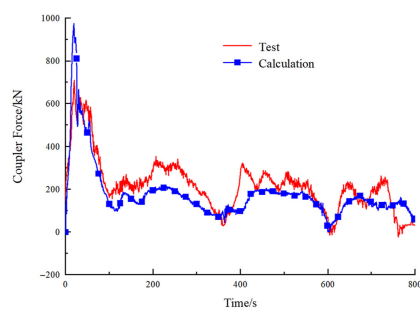The anterior coupler of
the 53rd vehicle

(a)

The anterior coupler of
the 104th vehicle

(b)
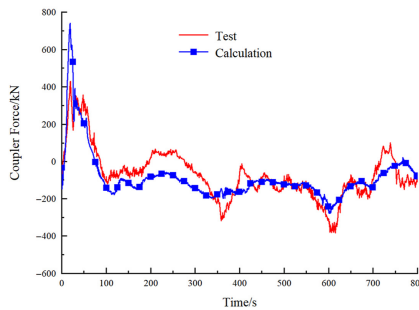
The anterior coupler of
the 131st vehicle

(c)

The anterior draft gear of the
164th vehicle

(d)

The anterior draft gear of the
280th vehicle

(e)

Source(s): Authors own work

4. Influence of longitudinal force

In the extreme-long train, the master locomotive and the first slave locomotive are HX_D1F-type electric locomotive with 30 t axle load while other slave locomotives are HX_N3-type diesel locomotive with 25 t axle load. The vehicles are C_{96}-type wagons with 30 t axle load. Every

two wagons are equipped with a group of traction rods. The wagon groups are connected with NO.16 and NO.17 couplers (with a coupler clearance of 9.5 mm) and equipped with HM-1 draft gear. The master and slave locomotives use wireless synchronous control technology for communication, and the control action of slave locomotives has 3s delay.

The formation is as follows when the traction mass of the trains is $(30{,}000 + n \times 10{,}000)$ t

$$HX_D 1F \,(master\,locomotive) + 84 \times C_{96} + HX_D 1F \,(slave\,locomotive) + 84 \times C_{96} + n$$
$$\times [2 \times HX_N 3 \,(slave\,locomotive) + 84 \times C_{96}]$$
$$+ HX_N 3 \,(slave\,locomotive) + 84 \times C_{96} + HX_N 3 \,(slave\,locomotive)$$

4.1 Influence of train formation on longitudinal force when braking at straight line section
According to the formation of the extreme-long train described above, calculating the influence of different train formation on longitudinal force under full service braking and emergency braking conditions for 40,000, 60,000, 80,000, 100,000 and 120,000 t trains when decelerating from 60 km/h on straight line. The maximum longitudinal compressive forces at coupler with respect to different formations are shown in Figure 4. It can be seen that the maximum compressive force fluctuates according to 10,000 t unit train groups, and the maximum compressive force of each 10,000 t unit train takes place in the middle; the maximum compressive force for 40,000–120,000 t trains is about 320 kN and takes place in the middle of the first 10,000 t unit train.

The distribution of the maximum longitudinal compressive force under emergency braking with respect to different formations is shown in Figure 5. It shows that the maximum compressive force of 40,000–120,000 t trains is about 800 kN and takes place at the 85th–95th vehicle; the maximum compressive force gradually oscillates down from the 95th to 500th vehicle and fluctuates according to 10,000 t unit train groups from the 500th to 1025th vehicle.

The formations of 40,000–120,000 t train have little impact on the maximum longitudinal compressive force under full service braking and emergency braking on the straight line. The
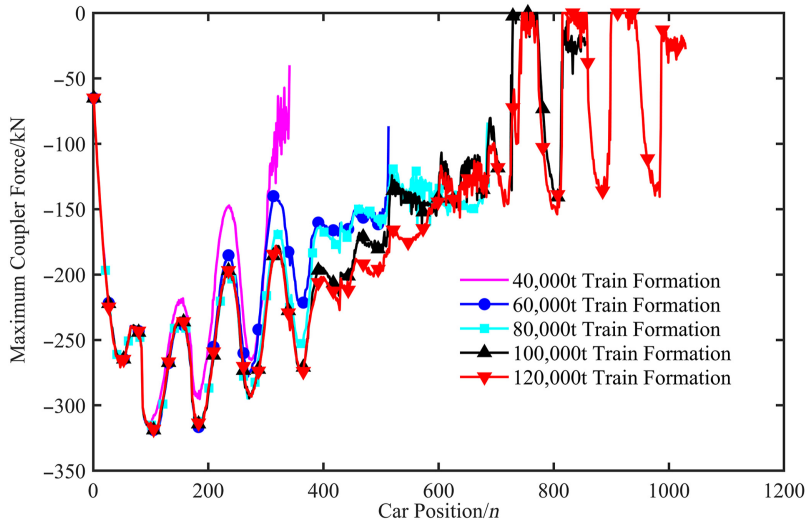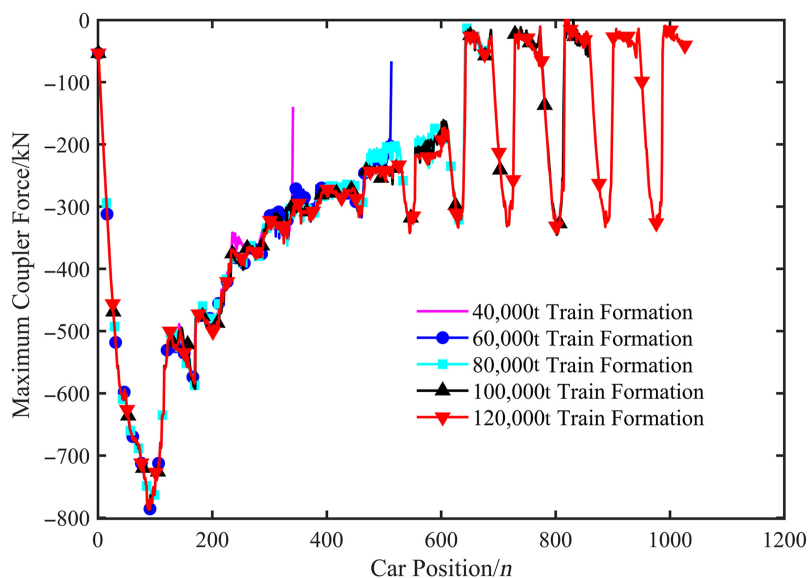

Figure 4.
Distribution of maximum force in different formations under full service braking

Source(s): Authors own work

Figure 5.
The distribution of
maximum coupler
force in different
formation length under
emergency braking

Source(s): Authors own work

main reason is that the action delay times of the slave locomotives are very close, which affects the speed of braking wave and braking force of the former two 10,000 t unit train groups.

4.2 Influence of time delay of wireless synchronous control on longitudinal force
LOCOTROL technology is used to control the synchronous response time between the master locomotive and slave locomotives. The wireless synchronous control delay time of slave locomotives is a key factor affecting the longitudinal force of extreme-long trains. Since the formation length of 40,000–120,000 t extreme-long train has little influence on the maximum longitudinal force of the train during emergency braking on the straight line, when analyzing the influence of the response delay time between the master and slave locomotives on the longitudinal force, its only necessary to calculate the effect on the longitudinal force under emergency braking at 60 km/h on the straight line for 40,000 t extreme-long trains with of 2, 3, 5 and 6s, respectively. The distribution of the maximum longitudinal coupler compressive force with each vehicle in emergency braking condition is shown in Figure 6.

It can be seen from Figure 6 that the maximum coupler compressive force of the train appears near the 90th vehicle, it reaches 1200 kN (the 92nd vehicle) when the delay time is 5s, and which is about 140% higher than 500kN with 2s; when the delay time is 6s, the maximum coupler compressive force reaches 1300kN, which does not exceed the safety limit of 2250kN in the Chinese standard Standard on Strength Design and Accreditation Test of Railway Vehicles (1996).

The variation of maximum longitudinal coupler compressive force with delay time under emergency braking of 40,000 t extreme-long trains is shown in Figure 7. It is shown from Figure 7 that the maximum coupler force grows approximately linearly with the increase of the wireless synchronous control delay time of slave locomotives, and the growth rate is $200 \, \text{kN} \cdot \text{s}^{-1}$.

4.3 Influence of gradient on longitudinal force
Due to the length of the extreme-long train and the line profile occupied by the train is complex; the line profile is also an important factor affecting the longitudinal force of the
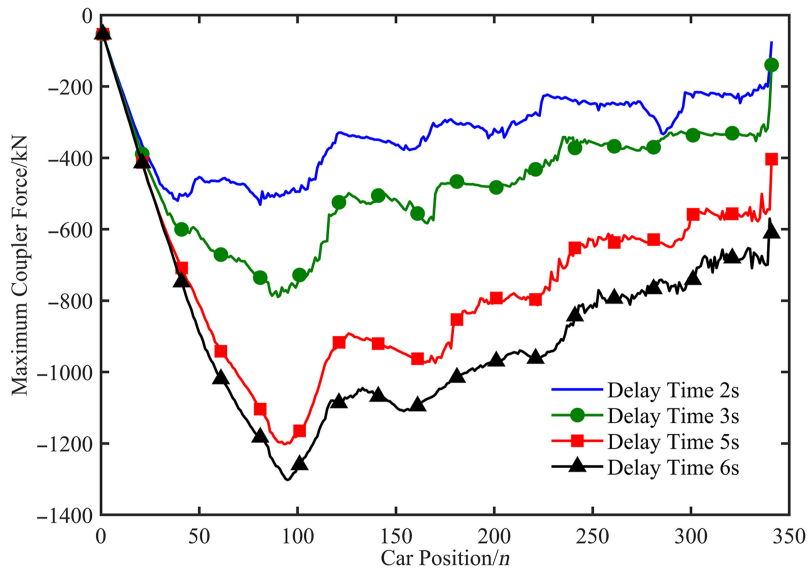
Figure 6.
The distribution of maximum coupler force in different delay time
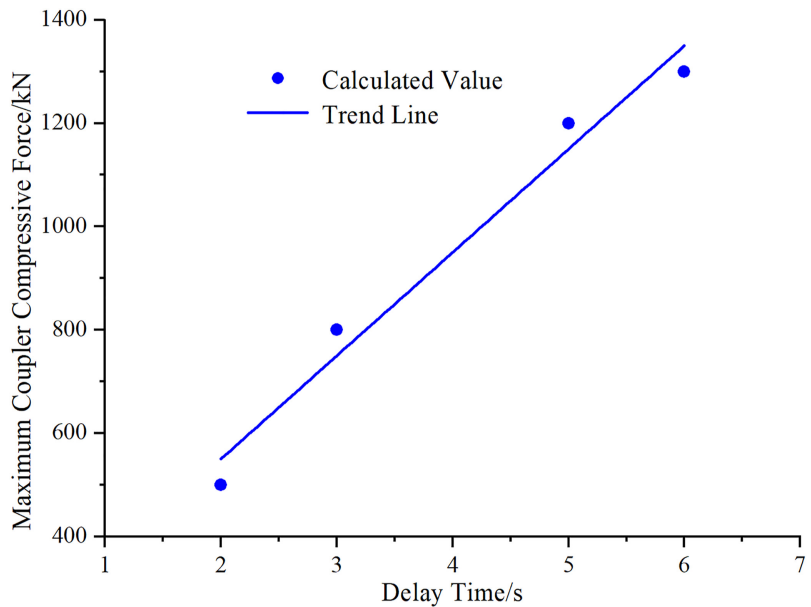
Source(s): Authors own work

Figure 7.
The variation of maximum coupler compressive force with delay time under emergency braking

Source(s): Authors own work

extreme-long train. Heavy-haul trains run from Northwest to Southeast of China as well as long and steep downhill line conditions are quite common.

In order to analyze the influence of the slope difference for the long and steep downhills on the longitudinal force with extreme-long trains, according to the extreme-long train formation mode described above, It's calculated that the influence of the slope difference on the longitudinal force with 40,000, 60,000, 80,000 and 100,000 t extreme-long trains under the full service braking condition when running at 60 km/h on the 13‰ downhill connecting 10‰, 8‰, 6‰ and 4‰ downhills and the straight line.

The distribution of maximum longitudinal coupler compressive force with 40,000 t extreme-long trains in various slope differences is shown in Figure 8. As can be seen from Figure 8: the maximum coupler force of extreme-long trains which appears in the 195th–201st vehicle is growing with the increase of slope difference on long and steep downhills; besides, the maximum coupler compressive force is 897kN and 2091kN when the slope differences are 3‰ and 13‰, respectively.

The maximum longitudinal coupler compressive force with 60,000 t train at various slope is shown in Figure 9. The maximum coupler force of the trains happens to the 284th ~ 290th vehicle is also growing with the slope difference on long and steep down-hills; when the slope difference is 9‰, the maximum coupler compressive force which reaches 2,350kN has exceeded the safety limit in the Chinese Standard on Strength Design and Accreditation Test of Railway Vehicles (1996), and the draft gear has been crushed.

The distribution of the maximum longitudinal coupler compressive force with 80,000 t extreme-long trains at different slope differences is shown in Figure 10. The maximum coupler force in the combined train which appears in the 378th–418th vehicle increases with the slope difference on the long and steep downhills; when the slope difference is 7‰, the maximum coupler compressive force which reaches 2400kN has exceeded the safety limit of 2,250kN in the Chinese Standard on Strength Design and Accreditation Test of Railway Vehicles (1996), and the draft gear has been crushed.

The distribution of maximum longitudinal coupler compressive force with each vehicle of 100,000 t extreme-long combined train at various slope differences is shown in Figure 11.
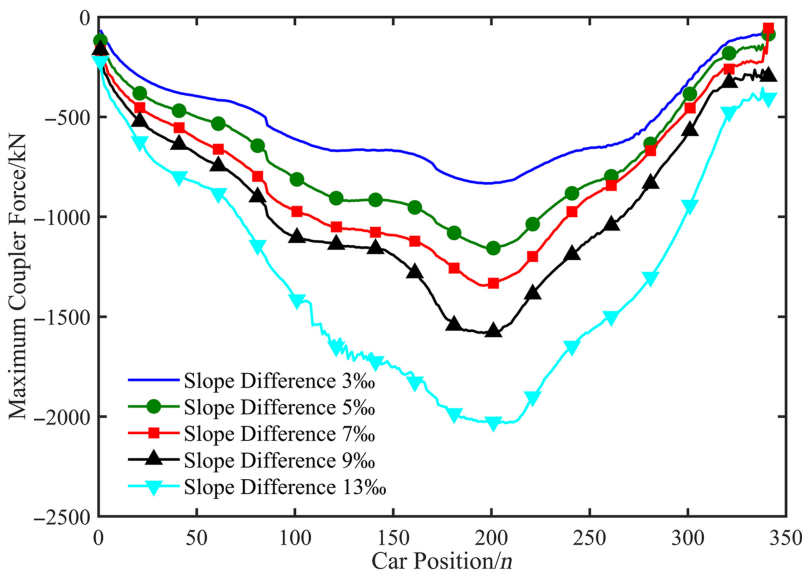

Figure 8.
The distribution of maximum coupler force with 40,000t extreme-long trains in various slope differences
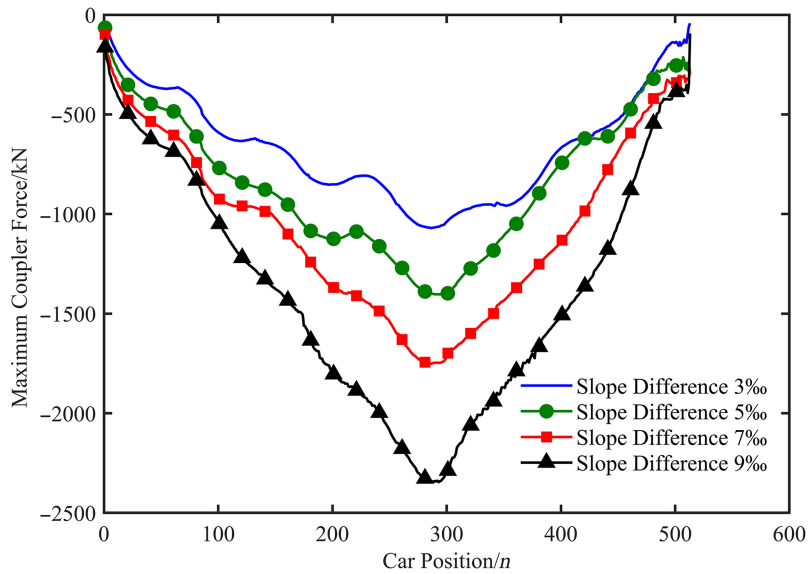
Source(s): Authors own work

Figure 9.
The distribution of
maximum coupler
force with 60,000t
extreme-long trains in
various slope
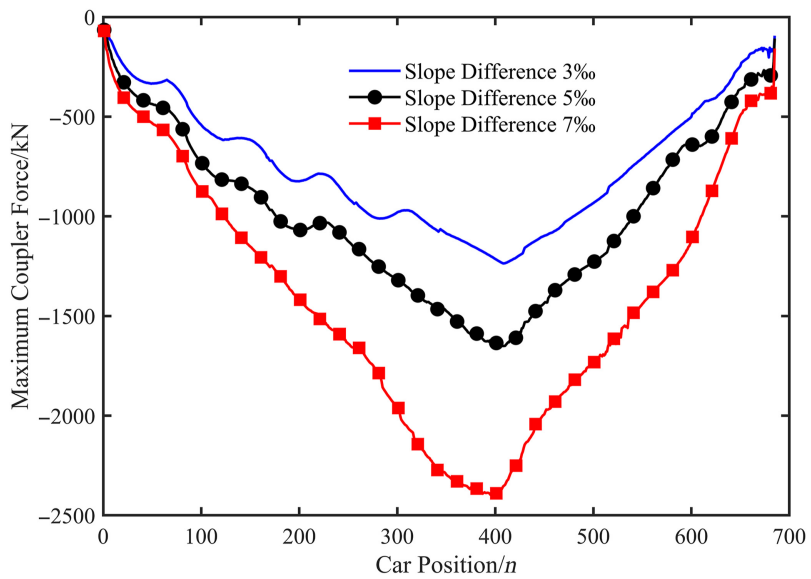differences
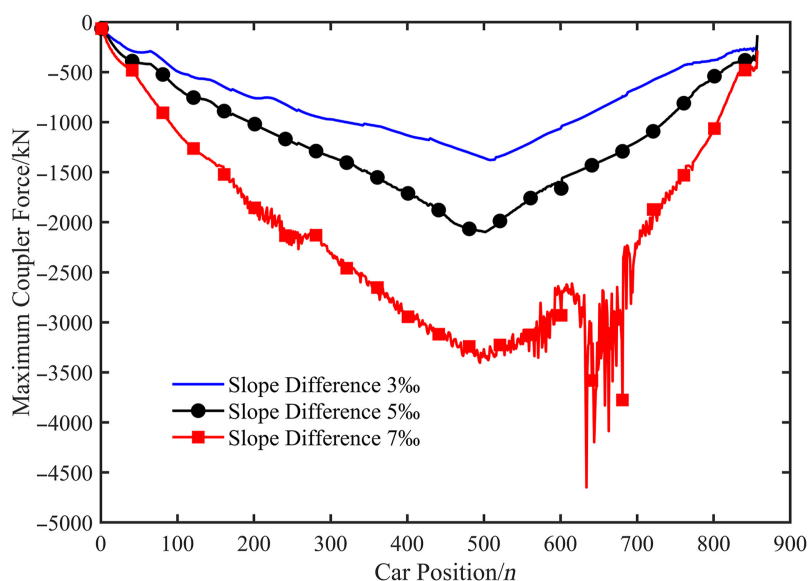
Source(s): Authors own work

Figure 10.
The distribution of
maximum coupler
force with 80,000t
extreme-long trains in
various slope
differences

Source(s): Authors own work

As can be seen from Figure 11: the maximum coupler compressive force in the combined train which appears near the 500th vehicle is also growing with the increase of the slope difference on the long and steep downhills; when the slope difference is 5‰, the maximum coupler

Source(s): Authors own work

compressive force reaches 2,099kN; when the slope difference exceeds 7‰, the maximum coupler compressive force exceeds the safety limit of 2,250kN in the Chinese Standard on Strength Design and Accreditation Test of Railway Vehicles (1996), and the draft gear has been crushed.

The relationship between the maximum longitudinal coupler compressive force of the train and the slope difference on the long and steep downhill under different formation lengths is shown in Figure 12. Figure 12 shows that the slope difference has a great impact on the maximum coupler force of the extreme-long train when 40,000–100,000 t extreme-long train runs under full service braking at 60 km/h on the long and steep downhill. The maximum coupler force of the train grows with the increase of the slope difference and the longer the train formation length is, the greater the increment of the coupler force is; the maximum coupler force of the train grows with the increase of formation length and the greater the slope difference is, the greater the increment of the coupler force is; for extreme-long trains with different formation lengths, the allowable maximum slope difference on the long and steep down-hill decreases with the increase of formation length in the condition that the maximum coupler force of the train does not exceed the safety limit of 2,250kN. The allowable maximum slope difference for 40,000 t extreme-long trains is 13‰ and there is only 5‰ slope difference for 100,000 t extreme-long trains.

4.4 Influence of coupler clearance on longitudinal force

New type of gapless couplers or traction rods can be used to better the longitudinal impulse between vehicles of extreme-long trains. When the 40,000 t combined train runs on 13‰ long and steep down-hill connecting with the straight line at 60 km/h under full service braking conditions, the distribution of the maximum longitudinal coupler compressive force of each vehicle under different coupler clearances is shown in Figure 13 by analyzing the influence of the general couplers (coupler clearance 9.5 mm), new type of gapless couplers and traction
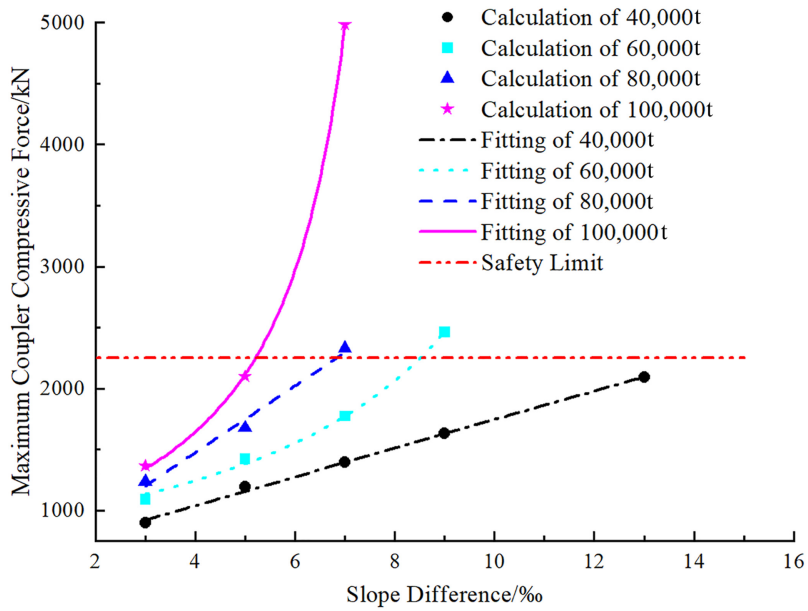
Figure 12.
The relationship
between the maximum
coupler force and the
slope difference in
different formation
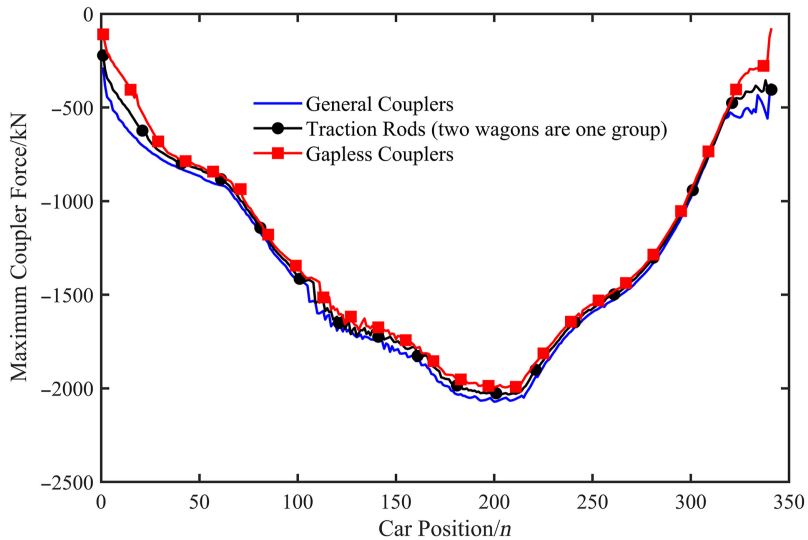length

Source(s): Authors own work

Figure 13.
The distribution of
maximum coupler
force in different
coupler clearances

Source(s): Authors own work

rods (two wagons are a group) on the longitudinal force. Figure 13 shows that the maximum coupler force is about 2070kN when using general couplers, using traction rods can reduce the maximum coupler force by about 2%, and using new type of gapless couplers can reduce the coupler force by about 4%.

4.5 Influence of ECP braking control technology on longitudinal force
The effect of ECP braking control technology on the longitudinal force is analyzed by simulating the full service braking and emergency braking conditions of 40,000 t extreme-long trains at 60 km/h on the 13‰ long and steep downhill section connecting the straight line, and the distribution of maximum coupler force under full service braking condition using ECP braking control technology and traditional LOCOTROL wireless synchronous control technology (delay time 3s) is obtained. As shown in Figure 14. It can be seen from Figure 14 that the decline of the maximum coupler force is not significant under the full service braking in the variable slope section when the extreme-long train adopts ECP braking technology.

The distribution of the maximum longitudinal coupler compressive force of each vehicle is shown in Figure 15 when the 40,000 t extreme-long train adopts ECP braking control technology and traditional LOCOTROL wireless synchronous control technology under emergency braking condition. Figure 15 shows that the maximum coupler force under emergency braking can be significantly reduced by using ECP braking technology for extreme-long trains in the variable slope section.

5. Conclusion

(1) Based on the simulation calculations of train operation using the braking test conditions of a 30,000 t combined train on the ramp, it was found that the calculation law of longitudinal forces for long and heavy trains is consistent with the experimental results. This validates the effectiveness of the longitudinal dynamics model and calculation method for long and heavy trains.

(2) Further research reveals that on straight tracks, when combined trains weighing from 40,000 to 120,000 t apply full service braking and emergency braking at a speed of 60 km/h, the maximum longitudinal coupler forces are approximately 320 kN and
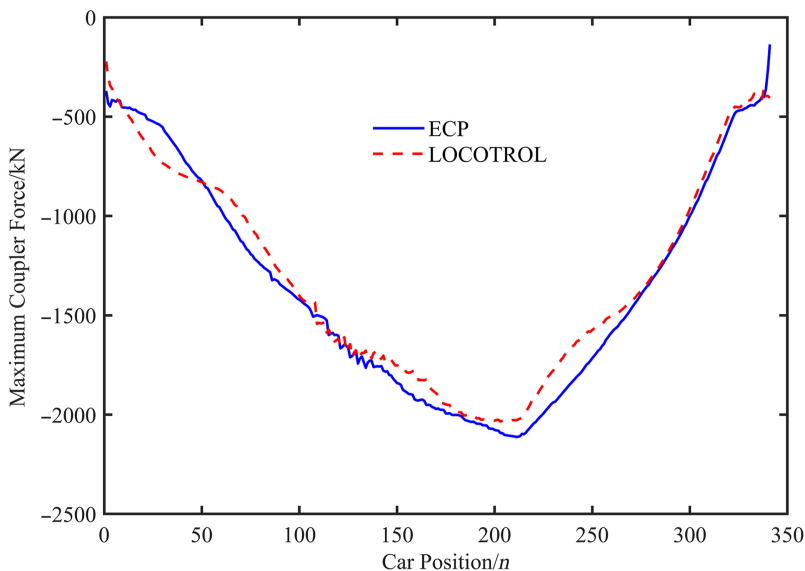
Figure 14.
The distribution of
maximum coupler
force in different
braking control
technologies under full
service braking
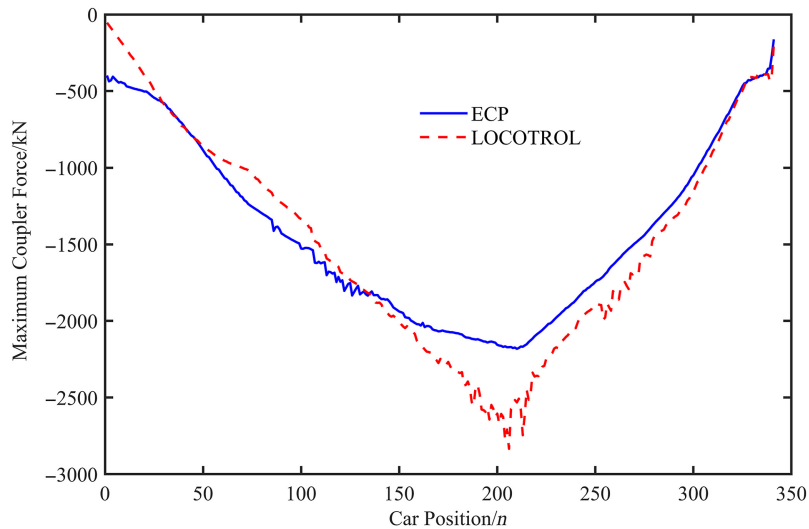
Source(s): Authors own work

Figure 15.
The distribution of
maximum coupler
force in different
braking control
technology under
emergency braking

Source(s): Authors own work

800 kN, respectively. These data reveal the levels of longitudinal forces experienced by extreme-long heavy-haul trains during braking on straight tracks.

(3) When the extreme long train on the straight line runs at 60 km/h with emergency braking effort applied, the maximum coupler force of the train grows with the increase of the wireless synchronous control delay time between the slave locomotives and the master locomotive. The maximum coupler force of the extreme long train reaches 1,200kN when the synchronous control delay time is 5s, which increases by about 140% compared with the delay time of 2s.

(4) On a 13% downhill gradient followed by a straight track, when combined trains with a total weight exceeding 40,000 t apply full braking at a speed of 60 km/h, the maximum longitudinal coupler force exceed the limit, posing serious safety hazards. This finding highlights the need for special attention to braking conditions on downhill gradients when designing and operating extreme-long heavy-haul trains.

(5) When combined trains weighing from 40,000 to 100,000 tons perform full braking at 60 km/h on downhill gradients, the allowable range of grade difference decreases as the train length increases. Particularly for a 100,000 ton combined train, the maximum allowable grade difference is only 5‰. This result provides important references for the operation planning and design of extreme-long heavy-haul trains on downhill gradients.

In conclusion, through in-depth research on the influence of longitudinal forces on extreme-long heavy-haul trains, this study provides new insights and methods for the design and operation of such trains, thereby enhancing safety, operational efficiency and track system design. This research is of great significance in promoting the development of heavy-haul transportation.

References

Chang, C., Wang, X., & Jiang, Y. (2016). Numerical model of steel friction and elasticity cement composite draft gear. *China Railway Science*, *37*(4), 83–88, In Chinese.

Chang, C., Guo, G., Wang, J., & Ya, M. (2017). Study on longitudinal force simulation of heavy-haul train. *Vehicle System Dynamics*, *55*(4), 571–582.

Cole, C. (2006). Longitudinal train dynamics. In Iwnicki, S. (Ed.), *Handbook of Railway Vehicle Dynamics* (pp. 239–278). Boca Raton: Taylor & Francis.

Fancher, P. S., Ervin, R. D., MacAdam, C. C., & Winkler, C. B. (1980). *Measurement and representation of truck leaf spring*. Ann Arbor: High: Safety Research Institute. The Univof Michigan.

Kaiwen, Z. (1990). *Brake*. Beijing: China Railway Press. In Chinese.

Ministry of Railways of the people's Republic of China (1996). *Standard on Strength design and accreditation test of railway vehicles*. Beijing: China Standard Press.

Ministry of Railways of the people's Republic of China (1998). *Regulations on railway train traction calculation*. Beijing: China Standard Press.

Newmark, N. M. (1959). A method of computation for structural dynamica. *Journal of Engineering Mechanics Division*, *85*, 67–94.

Sun, S., Li, F., Huang, Y., Hao, W., Tang, J., Xu, L. (2015). Study on dyanamic model of friction draft gear of heavy freight wagon. *Journal of the China Railway Society*, *37*(8), 17–23, In Chinese.

Wu, Q., Cole, C., Luo, S., & Spiryagin, M. (2014). A review of dynamics modelling of friction draft gear. *Vehicle System Dynamics*, *52*(6), 733–758.

Wu, Q., Spiryagin, M., & Cole, C. (2016). Longitudinal train dynamics: An overview. *Vehicle System Dynamics*, *54*(12), 1688–1714.

Wu, Q., Spiryagin, M., Cole, C., Chang, C., Guo, G., Sakalo, A., & Wei, W. (2018). International benchmarking of longitudinal train dynamics simulators: Results. *Vehicle System Dynamics*, *56*(3), 343–365.

Yang, J., Chang, C., Feng, Q., & Ma, D. (2010). Study on the key technical parameter of the locomotive draft gear in a heavy-haul combined train. *China Railway Science*, *31*(3), 76–81, In Chinese.

Yao, X. (2014). *Comprehensive test of 30000 ton combined train on datong-Qinhuangdao line*. Beijing: China Academy of Railway Sciences.

Zhai, W. (1990). The predictor-corrector skeme based on the Newmark integration algorithm for non-linear structral dynamic analyses. *Chinese Journal of Computational Mechanics*, *7*(2), 51–58, Chinese.

Zhai, W. (1996). Two simple fast integration methods for large-scale dynamic problems in engineering. *International Journal for Numerical Methods in Engineering*, *39*(24), 4199–4214.

Corresponding author
Chongyi Chang can be contacted at: chychang@163.com